

PAPER • OPEN ACCESS

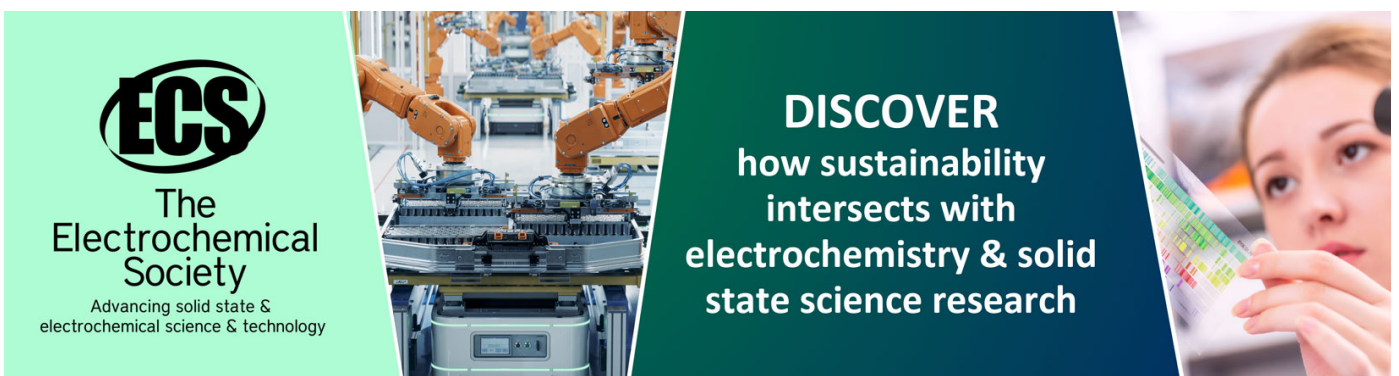
Dynamic characteristic study of composite box beam with corrugated webs considering interface slip and shear deformation

To cite this article: L Z Jiang *et al* 2018 *IOP Conf. Ser.: Earth Environ. Sci.* **189** 022015

View the [article online](#) for updates and enhancements.

You may also like

- [RING STAR FORMATION RATES IN BARRED AND NONBARRED GALAXIES](#)
R. D. Grouchy, R. J. Buta, H. Salo et al.
- [Limb-darkening Coefficients for the Filter CBB](#)
A. Claret, E. Mullen and B. L. Gary
- [A first-principles study on three-dimensional covalently-bonded hexagonal boron nitride nanoribbons](#)
Sang-Hoon Lee and Seung-Hoon Jhi



ECS
The
Electrochemical
Society
Advancing solid state &
electrochemical science & technology

DISCOVER
how sustainability
intersects with
electrochemistry & solid
state science research

Dynamic characteristic study of composite box beam with corrugated webs considering interface slip and shear deformation

L Z Jiang^{1,2}, X L Chai¹, Y L Feng¹, W B Zhou^{*1,2}, Y T Zhang¹, Z H Tan¹

¹ School of Civil Engineering, Central South University, Changsha 410075, China;

² National Engineering Laboratory for High Speed Railway Construction, Changsha 410075, China

Corresponding author, Professor, E-mail: zhouwangbao@163.com

Abstract. In order to study the effect of interface slip and shear deformation on the natural vibration of composite box girders with corrugated webs (CBBCW), based on the Hamilton principle, the effects of the slip, shear deformation and moment of inertia of CBBCW have been investigated. Further, the flexural vibration differential equations and natural boundary conditions of the CBBCW have been deduced. The formula for the flexural natural vibration frequency of CBBCW has been developed. The influencing rule of the interface slip stiffness and web shear deformation on the flexural natural vibration frequency of the CBBCW has been analyzed. The results of this study show that the analytical results are in good agreement with the results of the ANSYS finite element calculation, and some significant conclusions can be applied to the engineering design. The interface slip stiffness has some effect on the flexural natural vibration frequency of the CBBCW, and the maximum interface slip effect is up to 13.7%. The shear deformation has a significant effect on the natural vibration properties of the CBBCW, and the shear deformation effect increases significantly with the increase of the order of flexural natural vibration frequency. The formula has been developed further as compared with the earlier developed calculation theory for the flexural natural vibration of CBBCW. It can also provide a reference for future study of dynamic characteristics of CBBCW.

1. Introduction

The composite box girder with corrugated webs (CBBCW) is composed of concrete top slab, steel bottom slab and steel corrugated webs. Compared with the traditional steel-concrete composite beam, CBBCW has the following advantages: the corrugated webs has low axial stiffness and can greatly improve the efficiency of the applied prestress and reduce the shrinkage and creep effects of the concrete slabs. The corrugated web has a large out-of-plane stiffness and high shear buckling resistance. Moreover, it has a high local bearing capacity and anti-fatigue performance. In recent years, CBBCW has been widely used in the construction of buildings, roads, railways and urban rail transit [1-4].

Using the computer program ABAQUS, Elgaaly M et al.[5] performed a failure analysis of the beams with corrugated webs under shear. They found that the failure was due to the buckling of the webs. By carrying out elastic bifurcation buckling analyses using ABAQUS, Hassanein et al.[6, 7] presented the critical shear buckling stress of the corrugated webs of tapered bridge girders with steel corrugated webs, where the webs in different typologies of tapered girders with steel corrugated webs



were considered. Leblouba M [8] performed a series of three-point load tests on five shear-critical trapezoidal corrugated web beams. All the tested beams were observed to have a residual strength that was about half of their ultimate load carrying capacity regardless of the shear buckling mode. Experimental and theoretical studies on the shear buckling characteristics and the shear strength of trapezoidal corrugated steel webs had been conducted by Barakat S et al.[9], Leblouba M et al.[10], Sause R and Braxtan T N[11] and Nie J et al. [12]. Based on these studies, the analytical solutions for the elastic local and global buckling strengths have been deduced and some formulae for predicting the shear strength have also been developed. Elamary A et al. [13] conducted an experimental study to investigate the effect of a top steel flange on the failure mechanism of a steel-concrete composite beam with a corrugated web under bending. Zhou M et al.[14] conducted experimental and theoretical studies on the deformation of a non-prismatic scaled model with corrugated steel webs to quantify the proportional relationship between the bending deformation and shear deformation. He J et al.[15-17] tested seven steel and composite I-girders with corrugated webs to investigate the shear performance. In the tests, the parameters such as the thickness of steel web and shear connection degree between the steel web and encased concrete were examined. Through experimental and analytical studies, Nie J et al.[18] investigated the behavior of simply supported prestressed steel-concrete composite beams. They found that a partial composite design would result in a bigger interface slip at the steel-concrete interface. Eventually, this slip could lead to a bigger deflection. Even with a full composite design, the calculated deflection ignoring the interface slip was smaller than the experimental measured deflection. Further, in some cases (e.g. for steel-concrete composite beams with reduced span-to-depth ratio[19, 20]), it might not be appropriate to neglect the shear deformation in the beams, such as the Euler-Bernoulli beams (i.e. beams with infinite shear stiffness). Xu and Wu[21, 22] developed a new plane stress model of the composite steel-concrete beams with interlayer slips. Their study showed that the one-dimensional theory underestimated the deflection of the steel-concrete composite beams due to neglecting the shear deformation. Therefore, the natural vibration characteristics of steel-concrete composite beams were influenced by both effects of the shear deformation and the interface slip[23-26].

Zhou W et al.[27] derived and solved the flexural vibration equilibrium differential equations of the steel-concrete composite beams by taking the shear deformation and the interface slip into consideration. They found that effect of the interface slip on the flexural natural frequencies of the low mode orders was significant. Chen X et al.[28] developed a sandwich beam model for predicting the flexural vibration behavior of bridges with corrugated steel webs. In this model, the presence of diaphragms and interaction between the web shear deformation and flange local bending were considered. They found that the flexural natural frequencies and mode shapes obtained from the sandwich beam model and the Timoshenko models were basically the same. Based on the preceding literature review, it could be seen that there are only a few studies on the flexural natural vibration of CBBCW with comprehensive consideration of the shear deformation, interface slip and longitudinal inertia of motion.

In this study, based on the Hamilton principle, the effects of numerous factors, such as the interface slip, shear deformation, and moment of inertia of CBBCW on flexural natural vibration of the CBBCW have been investigated. Further, the governing differential equations and the natural boundary conditions of CBBCW have been deduced, and an analytical calculation method for the natural vibration characteristics of CBBCW considering the effects of shear deformation and interfacial slip has been developed. Finally, a number of examples of different boundary conditions and shear connection degrees have been used to compare the results of the analytic solution with those of the ANSYS finite element analysis.

2. Basic assumptions

The cross-sectional dimensions and coordinate system of a CBBCW are shown in Figure 1, and the longitudinal section is shown in Figure 2. To simplify the calculations, based on the characteristics of the CBBCW, the following assumptions have been made.

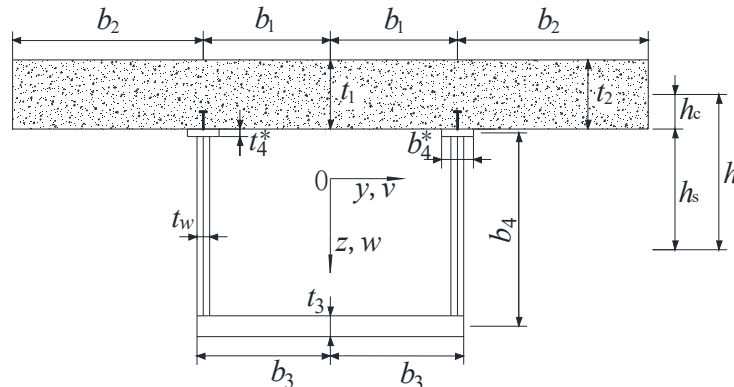


Figure 1. Cross-sectional dimensions of CBBCW and coordinate system

The longitudinal displacement of the CBBCW cross-section is superimposed by the longitudinal displacement based on the plane section assumption and the relative longitudinal slip caused by the flexibility of the shear connectors, whose expression is

$$u_{xi}(x, y, z, t) = k_c \xi(x, t) - (z - z_i) \theta(x, t) \quad i = 1, 2 \quad (1)$$

$$u_{xi}(x, y, z, t) = k_s \xi(x, t) - (z - z_s) \theta(x, t) \quad i = 3, 4 \quad (2)$$

From the literature [29, 30], we have

$$k_c = -A_s / A_0 \quad (3)$$

$$k_s = A_c / (nA_0) \quad (4)$$

where θ is the cross-section rotation of the CBBCW; $2b_1$, b_2 , $2b_3$, b_4 , b_4^* are the widths of the top concrete slab, cantilever slab and steel beam bottom plate, height of corrugated web, and width of the steel beam top flange, respectively; t_1 , t_2 , t_3 , t_w , t_4^* are the thicknesses of the top concrete slab, cantilever slab, steel beam bottom plate, corrugated web and steel beam top flange, respectively; z_i , z_b and z_s are the coordinates in z -direction of centroids of the concrete slab, steel beam bottom plate and steel beam; $n = E_s / E_c$ where E_s is the elastic modulus of the steel beam, and E_c is the elastic modulus of the concrete slab; $A_1 = 2b_1 t_1$; $A_2 = 2b_2 t_2$; $A_3 = 2b_3 t_3$; $A_4 = 2b_4 t_w$; $A_4^* = 2b_4^* t_4^*$; $A_0 = (A_1 + A_2) / n + A_3 + A_4^*$; $A_c = A_1 + A_2$ which is the cross-sectional area of the concrete slab, $A_s = A_3 + A_4^*$ which is the effective area of the steel beam cross-section, $\xi(x, t)$ is the longitudinal displacement difference between the concrete slab and the steel beam centroids.

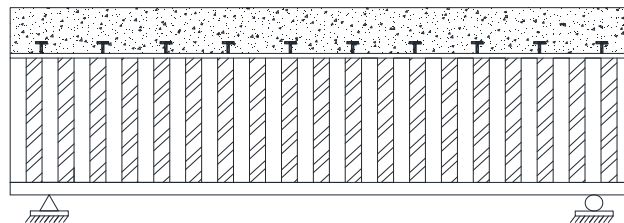


Figure 2. Longitudinal section of CBBCW

The vertical compressive deformation of the concrete slab and steel beam are small and negligible. The relative longitudinal slip between the slab and the beam $\zeta(x, t)$ can be determined from Eqs.(1)-(2) as follows:

$$\zeta(x, t) = \xi + h_c \theta + h_s \theta = \xi + h \theta \quad (5)$$

where h_c and h_s are the distances from the centroids of concrete slab and steel beam to the interface, respectively. Further, $h = h_c + h_s$.

If the linear elastic constitutive relationship of the concrete, steel and shear connectors is introduced, the shear stresses of the CBBCW shear connectors can be calculated using the following equations [18, 31]:

$$\zeta(x, t) = k_{sl} \zeta(x, t) = k_{sl} (\xi + h\theta) \quad (6)$$

$$V_u = A_s f_s r l_s / (L n_s) \quad (7)$$

$$k_1 = 0.66 n_s V_u \quad (8)$$

$$k_{sl} = k_1 / l_s \quad (9)$$

where V_u is the ultimate bearing capacity of a single stud; L is the span of the composite beam; r is the shear connector degree; f_s is the yield strength of the studs; k_1 is the slip stiffness of a single stud; n_s is the number of studs at each horizontal row; k_{sl} is the interface slip stiffness between the concrete slab and the steel beam; and l is the longitudinal spacing between the studs.

Since the axial deformation stiffness of the corrugated web is only a few hundredths or even a few thousandths of the axial deformation stiffness of a flat web of the same thickness, for simpler calculations, the axial deformation stiffness of the corrugated web has been neglected, i.e. the equivalent axial elastic modulus of the corrugated web has been taken as zero[32].

3. Governing differential equations and solution

3.1. Strain and stress expressions at each point

According to the longitudinal displacement expressions (Eqs. (1)-(5)), the strain expression at each point of the CBBCW cross-section is

$$\varepsilon_{xi} = k_c \frac{\partial \xi}{\partial x} - (z - z_i) \frac{\partial \theta}{\partial x} \quad i = 1, 2 \quad (10)$$

$$\varepsilon_{xi} = k_s \frac{\partial \xi}{\partial x} - (z - z_s) \frac{\partial \theta}{\partial x} \quad i = 3, 4 \quad (11)$$

$$\gamma_{xz} = \frac{\partial w}{\partial x} - \theta \quad (12)$$

where ε_i ($i = 1, 2, 3, 4$) are longitudinal normal strains of the top slab, cantilever slab and bottom slab, respectively; γ_{xz} is the shear strain of the corrugated web; and w is the vertical deflection of the CBBCW.

The stress at each point of the CBBCW cross-section is

$$\sigma_{xi} = E_c \left[k_c \frac{\partial \xi}{\partial x} - (z - z_i) \frac{\partial \theta}{\partial x} \right] \quad i = 1, 2 \quad (13)$$

$$\sigma_{xi} = E_s \left[k_s \frac{\partial \xi}{\partial x} - (z - z_s) \frac{\partial \theta}{\partial x} \right] \quad i = 3 \quad (14)$$

$$\sigma_{x4} = E_e \left[k_s \frac{\partial \xi}{\partial x} - (z - z_s) \frac{\partial \theta}{\partial x} \right] = 0 \quad (15)$$

$$\tau_{xz} = G_e \left(\frac{\partial w}{\partial x} - \theta \right) \quad (16)$$

where G_e is the equivalent shear modulus of the the corrugated web; E_e is the equivalent axial elastic modulus of the corrugated web (i.e. $E_e = 0$); σ_{xi} ($i = 1, 2, 3$) are the longitudinal normal stresses of the concrete top slab, cantilever slab and bottom slab, respectively; and τ_{xz} is the shear stress of the corrugated web.

3.2. Equivalent shear modulus of the corrugated web

The longitudinal unit cross-section of the corrugated web is shown in Figure 3. The equivalent shear modulus of the corrugated web is smaller than that of the flat web, and its equivalent shear modulus can be calculated using the following equation [33]:

$$G_e = G_s \frac{b_w + d_w}{b_w + d_w \sec \theta_w} \quad (17)$$

where G_s is the elastic modulus of steel; as shown in Figure 3, h_w is the wave height of the corrugated web; b_w , d_w and b_{w1} are the length of the straight section of the corrugated web, the projection length of the inclined plate section on the horizontal line and the length of the inclined plate section, respectively; and θ_w is the bevel angle of corrugated web.

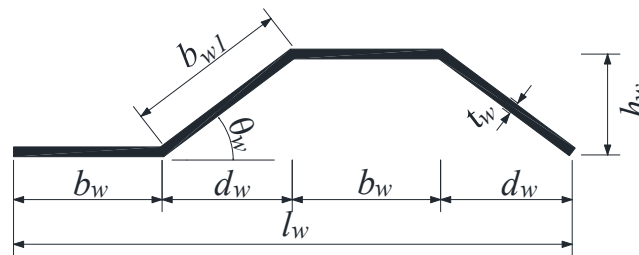


Figure 3. A cross-section of longitudinal unit of corrugated web

3.3. Flexural vibration differential equations and natural boundary conditions of CBBCW

The strain energy of the CBBCW is

$$V = \frac{1}{2} \int_L \left[\sum_{i=1}^4 \int_{A_i} (\sigma_{xi} \epsilon_{xi} + \tau_{xyi} r_{xyi} + \tau_{xzi} r_{xzi}) dA + \zeta \zeta' \right] dx \quad (18)$$

Substituting Eqs. (5)-(16) into Eq. (18) gives

$$V = \frac{1}{2} \int_L \left[D \xi'^2 - 2J \xi' \theta' + I \theta'^2 + \zeta \zeta' + G_e A_4 (w' - \theta)^2 \right] dx \quad (19)$$

where “ \cdot ” and “ $'$ ” represent the partial derivatives with respect to time t and coordinate x , respectively. $D = E_c k_c^2 A_c + E_s k_s^2 (A_{4*} + A_3)$; $J = k_c E_c J_c + k_s E_s J_s$; $I = E_c I_c + E_s I_s$; $J_c = \int_{A_c} (z - z_i) dA$;

$$J_s = \int_{A_{4*} + A_3} (z - z_s) dA; I_c = \int_{A_c} (z - z_i)^2 dA; \text{ and } I_s = \int_{A_{4*} + A_3} (z - z_s)^2 dA.$$

As shown in Figure 3, the mass of a longitudinal unit of the corrugated web is:

$$m_4 = 2(b_{w1} t_w + b_w t_w) b_4 \rho_s \quad (20)$$

According to the principle of equivalent mass, the equivalent thickness of the corrugated web is:

$$t_{weq} = m_4 / (l_w b_4 \rho_s) \quad (21)$$

After considering the effect of moment of inertia, the total kinetic energy of the CBBCW can be expressed as

$$T = \frac{1}{2} \int_L m \dot{w}^2 dx + \frac{1}{2} \int_L \sum_{i=1}^4 \int_{A_i} \rho_i \dot{u}_i^2 dA dx \quad (22)$$

where $m = \rho_c A_c + \rho_s (A_s + A_{eq})$; $\rho_1 = \rho_2 = \rho_c$; $\rho_3 = \rho_4 = \rho_4^* = \rho_{eq} = \rho_s$; ρ_c is the density of concrete; ρ_s is the density of steel; and $A_{eq} = t_{weq} b_4$ which is the equivalent cross-sectional area of the corrugated web.

Substituting Eqs. (5)-(16) into Eq. (22) gives

$$T = \frac{1}{2} \int_L (D_1 \dot{\xi}^2 - 2J_1 \dot{\xi} \dot{\theta} + I_1 \dot{\theta}^2) dx + \frac{1}{2} \int_L m \dot{w}^2 dx \quad (23)$$

$$\text{where } D_1 = \rho_c k_c^2 A_c + \rho_s k_s^2 (A_{4*} + A_4 + A_3) \quad ; \quad J_1 = \rho_c k_c J_c + \rho_s k_s J_s \quad ; \quad I_1 = \rho_c I_c + \rho_s I_s \quad ; \\ J_s = \int_{A_{4*} + A_4 + A_3} (z - z_s) dA \quad ; \quad I_s = \int_{A_{4*} + A_4 + A_3} (z - z_s)^2 dA.$$

According to the Hamilton principle, i.e. $\delta \int_{t_0}^{t_1} (T - V) dt = 0$, which can derive the flexural vibration differential equations and the natural boundary conditions of the CBBCW, as follows[34]:

$$D\xi'' - J\theta'' - k_{sl}\zeta - D_1\ddot{\xi} + J_1\ddot{\theta} = 0 \quad (24)$$

$$G_{s1}A_4(w'' - \theta') - m\ddot{w} = 0 \quad (25)$$

$$J_1\ddot{\xi} - I_1\ddot{\theta} + G_{s1}A_4(w' - \theta) - J\xi'' + I\theta'' - k_{sl}\zeta h = 0 \quad (26)$$

$$(D\xi' - J\theta')\delta\xi|_0^L = 0 \quad (27)$$

$$G_{s1}A_4(w' - \theta)\delta w|_0^L = 0 \quad (28)$$

$$(-J\xi' + I\theta')\delta\theta|_0^L = 0 \quad (29)$$

3.4. Solution of flexural natural vibration frequencies of CBBCW

Let

$$\xi(x, t) = \xi_1(x) \sin(\omega t + \varphi) \quad (30)$$

$$w(x, t) = w_1(x) \sin(\omega t + \varphi) \quad (31)$$

$$\theta(x, t) = \theta_1(x) \sin(\omega t + \varphi) \quad (32)$$

$$\lambda^k = \frac{\partial^k}{\partial x^k} \quad (33)$$

Substituting Eqs. (30)-(33) into Eqs. (24)-(26) gives

$$(D\lambda^2 - k_{sl} + D_1\omega^2)\xi_1 + (-J\lambda^2 - J_1\omega^2 - k_{sl}h)\theta_1 = 0 \quad (34)$$

$$(G_{s1}A_4\lambda^2 + m\omega^2)w_1 - G_{s1}A_4\lambda\theta_1 = 0 \quad (35)$$

$$(-J_1\omega^2 - J\lambda^2 - k_{sl}h)\xi_1 + G_{s1}A_4\lambda w_1 + (I_1\omega^2 - G_{s1}A_4 + I\lambda^2 - k_{sl}h^2)\theta_1 = 0 \quad (36)$$

The eigen equations correspond to Eqs. (34)-(36) can be shown as follows:

$$\begin{vmatrix} D\lambda^2 - k_{sl} + D_1\omega^2 & 0 & -J\lambda^2 - J_1\omega^2 - k_{sl}h \\ 0 & G_{s1}A_4\lambda^2 + m\omega^2 & -G_{s1}A_4\lambda \\ -J_1\omega^2 - J\lambda^2 - k_{sl}h & G_{s1}A_4\lambda & I_1\omega^2 - G_{s1}A_4 + I\lambda^2 - k_{sl}h^2 \end{vmatrix} = 0 \quad (37)$$

where $||$ denotes the determinant of a matrix.

The solution of the flexural vibration differential equations can be expressed as:

$$\xi_1 = \sum_{i=1}^6 a_i \beta_{1i} \exp(\lambda_i x) \quad (38)$$

$$w_1 = \sum_{i=1}^6 a_i \beta_{2i} \exp(\lambda_i x) \quad (39)$$

$$\theta_1 = \sum_{i=1}^6 a_i \beta_{3i} \exp(\lambda_i x) \quad (40)$$

$$\beta_{1i} = \frac{-(-J\lambda^2 - J_1\omega^2 - k_{sl}h)}{(D\lambda^2 - k_{sl} + D_1\omega^2)}, i = 1, 2, \dots, 6 \quad (41)$$

$$\beta_{2i} = \frac{G_{s1}A_4\lambda}{(G_{s1}A_4\lambda^2 + m\omega^2)}, i = 1, 2, \dots, 6 \quad (42)$$

$$\beta_{3i} = 1, i = 1, 2, \dots, 6 \quad (43)$$

where $\{a\} = \{a_1, a_2, \dots, a_6\}^T$ is a constant vector from the integration; and λ_i is eigen value of the eigen equations.

Eqs. (27)-(29) result in the common boundary conditions as follows:

The natural boundary condition for a simply supported end is:

$$\xi'_1 = 0, w_1 = 0, \theta'_1 = 0 \quad (44)$$

The natural boundary condition for a fixed supported end is:

$$\xi_1 = 0, w_1 = 0, \theta_1 = 0 \quad (45)$$

For the boundary conditions in Eqs. (44) and (45), the CBBCW has three natural boundary conditions at both ends. Substituting Eqs. (38)-(40) into the boundary conditions gives:

$$[B(\omega)]\{a\} = 0 \quad (46)$$

In Eq. (46), the integral constant vector must have a nonzero solution. Hence, the following requirement applies:

$$|B(\omega)| = 0 \quad (47)$$

Solving algebraic Eq. (47) gives the flexural natural vibration frequencies of the CBBCW.

4. Solution of natural frequencies of CBBCW without considering the shear deformation effect

The longitudinal displacement of the CBBCW cross-section at each point without considering the effect of the shear deformation is as follows:

$$u_{xi}(x, y, z, t) = k_c \xi(x, t) - (z - z_i) w'(x, t) \quad i = 1, 2 \quad (48)$$

$$u_{xi}(x, y, z, t) = k_s \xi(x, t) - (z - z_s) w'(x, t) \quad i = 3, 4 \quad (49)$$

From Eqs. (48)-(49), the longitudinal strain and stress expressions at each point of the CBBCW cross-section are as follows:

$$\varepsilon_{xi} = k_c \frac{\partial \xi}{\partial x} - (z - z_i) \frac{\partial^2 w}{\partial x^2} \quad i = 1, 2 \quad (50)$$

$$\varepsilon_{xi} = k_s \frac{\partial \xi}{\partial x} - (z - z_s) \frac{\partial^2 w}{\partial x^2} \quad i = 3, 4 \quad (51)$$

$$\sigma_{xi} = E_c \left[k_c \frac{\partial \xi}{\partial x} - (z - z_i) \frac{\partial^2 w}{\partial x^2} \right] \quad i = 1, 2 \quad (52)$$

$$\sigma_{xi} = E_s \left[k_s \frac{\partial \xi}{\partial x} - (z - z_s) \frac{\partial^2 w}{\partial x^2} \right] \quad i = 3 \quad (53)$$

$$\sigma_{x4} = E_e \left[k_s \frac{\partial \xi}{\partial x} - (z - z_s) \frac{\partial^2 w}{\partial x^2} \right] = 0 \quad (54)$$

According to Assumption (2), after neglecting the vertical compressive deformation of concrete and steel girder, the relative longitudinal slip between the concrete slab and the steel beam is reduced to:

$$\zeta(x, t) = \xi + hw' \quad (55)$$

According to the Hamilton principle $\delta \int_0^{t_1} (T - V) dt = 0$, the differential equations and the boundary conditions of the CBBCW without considering the shear deformation are as follows:

$$D\xi'' - Jw''' - k_{sl}(\xi + hw') - D_1\xi + J_1\ddot{w}' = 0 \quad (56)$$

$$J_1\ddot{\xi} - I_1\ddot{w}' - J\xi'' + Iw''' - k_{sl}h\xi + k_{sl}h^2w' + m\dot{w}' = 0 \quad (57)$$

$$(D\xi' - Jw'')\delta\xi|_0^L = 0 \quad (58)$$

$$(J_1\ddot{\xi} - I_1\ddot{w}' - J\xi'' + Iw''' - k_{sl}\zeta h)\delta w|_0^L = 0 \quad (59)$$

$$(-J\xi' + Iw'')\delta w|_0^L = 0 \quad (60)$$

The method of solving flexural natural vibration frequency of the CBBCW without considering the effect of shear deformation is the same as that described in Section 3.

5. Examples

Simply supported CBBCW beams and fixed end CBBCW beams of two different spans have been used as examples. The spans are $L_1 = 14m$ and $L_2 = 16m$. For the beams in each span, there are five different shear connection degrees, i.e. 0.25, 0.40, 0.60, 0.80 and 1.00. The mechanical and geometrical properties of the CBBCW beams are

$$E_s = 2.0 \times 10^{11} \text{ N} \cdot \text{m}^{-2}, E_c = 4.5 \times 10^{10} \text{ N} \cdot \text{m}^{-2}, \mu_s = 0.30, \mu_c = 0.18, \rho_s = 7870 \text{ kg} \cdot \text{m}^{-3}, \rho_c = 2570 \text{ kg} \cdot \text{m}^{-3},$$

$$b_1 = 0.4m, b_4 = 0.4m, b_2 = 0.2m, b_3 = 0.5m, b_5 = 0.2m, t_1 = t_2 = 0.12m, t_3 = t_5 = 0.025m, t_w = 0.005m,$$

$$h_w = 0.1m, b_w = 0.125m, d_w = 0.125m, b_{w1} = \sqrt{d_w^2 + h_w^2}$$

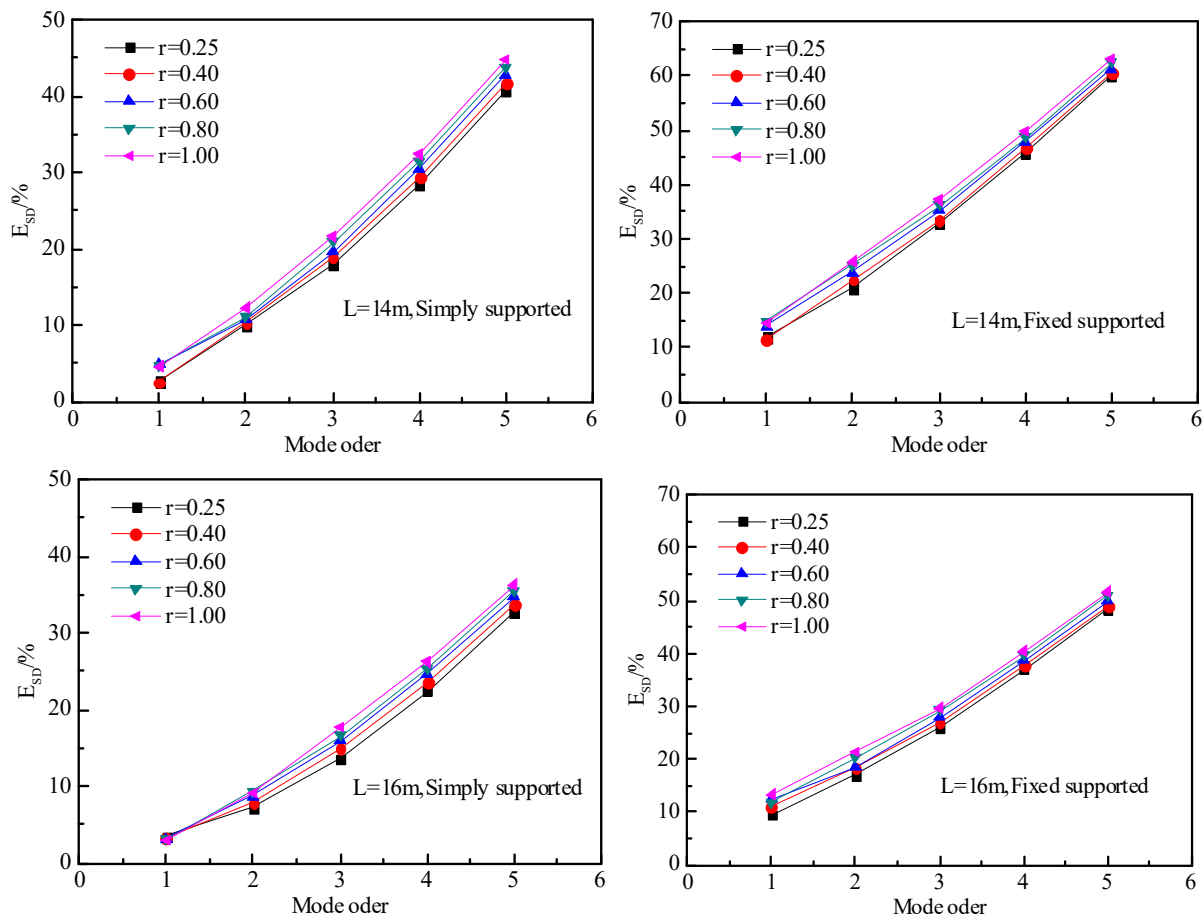


Figure 4. Relationship between the shear deformation effect and the mode orders of flexural natural vibration

In order to verify the practicability of the theoretical model in Section 3, ANSYS finite element method was used to carry out the simulations. The SOLID65 element was used to simulate the concrete slab, the SHELL43 element was used to simulate the steel beam and COMBIN14 element was used to simulate the studs. The simulation results are compared with the theoretical results as shown in Table 1-4 and Figures 4-5. R_{AN} denotes the ANSYS finite element calculation results; R_{SD} denotes the theoretical calculation results not considering the shear deformation effect; and R_{SS}

denotes the theoretical calculation results after comprehensive consideration of shear deformation and slip effect. The error of the theoretical calculation has been calculated using $E_{SS} = 100(R_{SS} - R_{AN})/R_{AN}$; the shear deformation effect has been calculated using $E_{SD} = 100(R_{SD} - R_{FB})/R_{FB}$; and the interface slip effect has been calculated using $E_{SL} = 100(R_{SS}|_{r=1.0} - R_{SS}|_{r=0.25})/R_{E}|_{r=1.0}$. From Table 1-4 and Figures 4-5, it can be seen that:

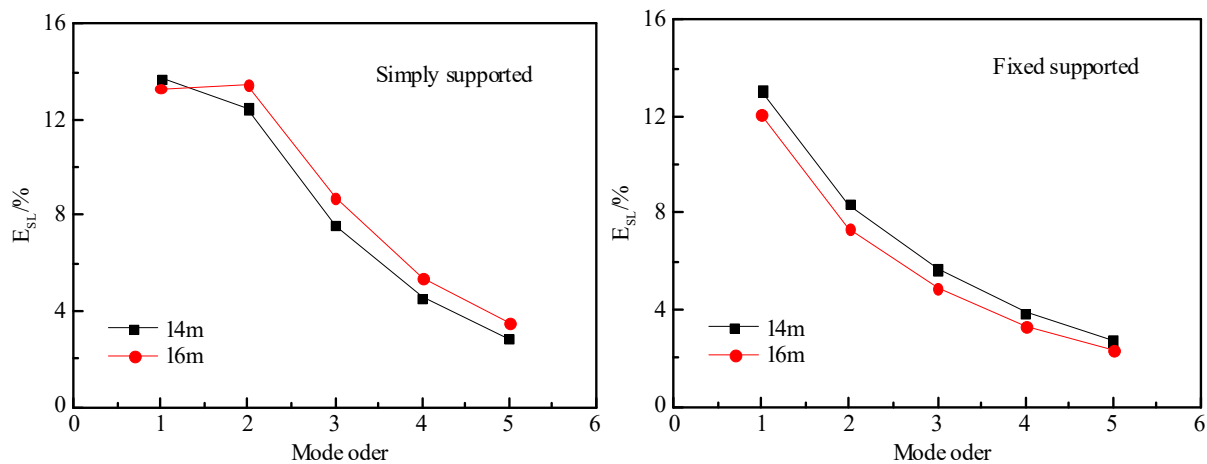


Figure 5. Relationship between the interface slip effect and the mode orders of flexural natural vibration

Table1. Comparison between calculation results of the ANSYS model and the analytical model (L=14m, simply supported)

<i>r</i>	Calculation methods	Natural frequencies/Hz				
		1st	2nd	3rd	4th	5th
0.25	R_{SD}	6.21	21.16	44.88	77.66	119.67
	R_{SS}	6.05	19.26	38.03	60.47	84.98
	R_{AN}	6.09	19.45	37.87	59.30	82.25
	$E_{SD}/\%$	2.63	9.92	17.99	28.42	40.82
	$E_{SS}/\%$	-0.76	-1.02	0.44	1.97	3.31
0.40	R_{SD}	6.52	22.12	46.15	79.09	121.10
	R_{SS}	6.37	20.05	38.83	61.11	85.46
	R_{AN}	6.40	20.14	38.57	59.92	82.77
	$E_{SD}/\%$	2.50	10.32	18.85	29.43	41.71
	$E_{SS}/\%$	-0.56	-0.42	0.66	1.98	3.24
0.60	R_{SD}	6.84	23.07	47.58	80.84	123.01
	R_{SS}	6.52	20.85	39.78	61.90	86.09
	R_{AN}	6.65	20.86	39.40	60.68	83.43
	$E_{SD}/\%$	4.88	10.69	19.60	30.59	42.88
	$E_{SS}/\%$	-1.95	-0.04	0.97	2.01	3.19
0.80	R_{SD}	7.00	23.87	48.85	82.43	124.76
	R_{SS}	6.68	21.48	40.42	62.70	86.73
	R_{AN}	6.82	21.42	40.11	61.37	84.04
	$E_{SD}/\%$	4.76	11.11	20.87	31.47	43.85
	$E_{SS}/\%$	-1.95	0.29	0.76	2.16	3.20

1.00	R_{SD}	7.16	24.67	50.13	83.86	126.35
	R_{SS}	6.84	21.96	41.22	63.34	87.21
	R_{AN}	6.93	21.88	40.74	62.00	84.61
	$E_{SD}/\%$	4.65	12.32	21.62	32.41	44.89
	$E_{SS}/\%$	-1.25	0.37	1.18	2.15	3.07
	$E_{SL}/\%$	13.71	12.47	7.58	4.55	2.86

Table 2. Comparison between calculation results of the ANSYS model and the analytical model (L=14m, fixed supported)

r	Calculation methods	Natural frequencies/Hz				
		1st	2nd	3rd	4th	5th
0.25	R_{SD}	11.94	31.19	59.68	97.23	144.28
	R_{SS}	10.66	25.78	44.88	66.68	90.07
	R_{AN}	10.81	26.02	45.43	67.41	91.02
	$E_{SD}/\%$	11.94	20.99	32.98	45.82	60.19
	$E_{SS}/\%$	-1.33	-0.93	-1.21	-1.09	-1.04
0.40	R_{SD}	12.41	32.15	60.79	98.50	145.13
	R_{SS}	11.14	26.26	45.51	67.15	90.39
	R_{AN}	11.17	26.51	45.96	67.92	91.48
	$E_{SD}/\%$	11.43	22.42	33.57	46.68	60.56
	$E_{SS}/\%$	-0.27	-0.94	-0.97	-1.12	-1.19
0.60	R_{SD}	13.05	33.10	62.22	100.10	146.88
	R_{SS}	11.46	26.73	45.99	67.63	91.02
	R_{AN}	11.56	27.06	46.59	68.54	92.05
	$E_{SD}/\%$	13.89	23.81	35.29	48.00	61.36
	$E_{SS}/\%$	-0.85	-1.20	-1.30	-1.32	-1.12
0.80	R_{SD}	13.53	34.05	63.49	101.53	148.47
	R_{SS}	11.78	27.21	46.63	68.27	91.34
	R_{AN}	11.86	27.53	47.16	69.11	92.59
	$E_{SD}/\%$	14.86	25.15	36.18	48.72	62.54
	$E_{SS}/\%$	-0.72	-1.16	-1.12	-1.22	-1.35
1.00	R_{SD}	13.84	34.85	64.61	102.96	149.90
	R_{SS}	12.09	27.69	47.10	68.75	91.82
	R_{AN}	12.11	27.94	47.66	69.64	93.10
	$E_{SD}/\%$	14.47	25.86	37.16	49.77	63.26
	$E_{SS}/\%$	-0.12	-0.89	-1.17	-1.28	-1.37
	$E_{SL}/\%$	12.06	7.36	4.92	3.30	2.29

Table 3. Comparison between calculation results of the ANSYS model and the analytical model (L=16m, simply supported)

r	Calculation methods	Natural frequencies/Hz				
		1st	2nd	3rd	4th	5th
0.25	R_{SD}	4.77	16.39	34.53	59.83	92.14

	R_{SS}	4.61	15.28	30.39	48.85	69.38
	R_{AN}	4.78	15.38	30.34	48.22	67.78
	$E_{SD}/\%$	3.45	7.29	13.61	22.48	32.80
	$E_{SS}/\%$	-3.41	-0.68	0.19	1.32	2.36
0.40	R_{SD}	5.09	17.19	35.65	61.11	93.41
	R_{SS}	4.93	15.91	31.03	49.49	69.86
	R_{AN}	5.02	15.98	31.00	48.83	68.31
	$E_{SD}/\%$	3.23	8.00	14.87	23.47	33.71
	$E_{SS}/\%$	-1.69	-0.40	0.11	1.36	2.27
0.60	R_{SD}	5.25	17.98	36.92	62.54	95.00
	R_{SS}	5.09	16.55	31.83	50.13	70.50
	R_{AN}	5.21	16.60	31.76	49.56	68.97
	$E_{SD}/\%$	3.12	8.65	16.00	24.76	34.76
	$E_{SS}/\%$	-2.27	-0.28	0.20	1.14	2.22
0.80	R_{SD}	5.41	18.62	38.03	63.81	96.44
	R_{SS}	5.25	17.03	32.62	50.92	71.13
	R_{AN}	5.33	17.07	32.41	50.22	69.57
	$E_{SD}/\%$	3.03	9.35	16.59	25.31	35.57
	$E_{SS}/\%$	-1.49	-0.26	0.65	1.39	2.25
0.80	R_{SD}	5.57	19.10	38.99	65.09	97.87
	R_{SS}	5.41	17.50	33.10	51.56	71.77
	R_{AN}	5.41	17.45	32.98	50.83	70.13
	$E_{SD}/\%$	2.94	9.09	17.79	26.23	36.36
	$E_{SS}/\%$	-0.06	0.29	0.37	1.45	2.33
	$E_{SL}/\%$	13.31	13.47	8.71	5.41	3.47

Table 4. Comparison between calculation results of the ANSYS model and the analytical model (L=16m, fixed supported)

r	Calculation methods	Natural frequencies/Hz				
		1st	2nd	3rd	4th	5th
0.25	R_{SD}	9.23	24.03	45.99	74.79	110.60
	R_{SS}	8.43	20.53	36.44	54.58	74.47
	R_{AN}	8.54	20.81	36.76	55.13	75.11
	$E_{SD}/\%$	9.43	17.05	26.20	37.03	48.50
	$E_{SS}/\%$	-1.21	-1.33	-0.87	-0.99	-0.85
0.40	R_{SD}	9.71	24.82	46.94	75.91	111.71
	R_{SS}	8.75	21.01	36.92	55.06	74.95
	R_{AN}	8.86	21.25	37.26	55.62	75.56
	$E_{SD}/\%$	10.91	18.18	27.16	37.86	49.04
	$E_{SS}/\%$	-1.18	-1.16	-0.92	-1.00	-0.80
0.60	R_{SD}	10.18	25.62	48.06	77.18	113.14
	R_{SS}	9.07	21.64	37.56	55.70	75.43
	R_{AN}	9.19	21.76	37.86	56.21	76.12

	$E_{SD} / \%$	12.28	18.38	27.97	38.57	50.00
	$E_{SS} / \%$	-1.29	-0.52	-0.80	-0.92	-0.91
0.80	R_{SD}	10.50	26.42	49.17	78.45	114.58
	R_{SS}	9.39	21.96	38.03	56.17	75.91
	R_{AN}	9.45	22.18	38.38	56.76	76.65
	$E_{SD} / \%$	11.86	20.29	29.29	39.66	50.94
	$E_{SS} / \%$	-0.60	-0.99	-0.90	-1.02	-0.97
1.00	R_{SD}	10.82	27.05	49.97	79.57	115.85
	R_{SS}	9.55	22.28	38.51	56.65	76.38
	R_{AN}	9.65	22.55	38.85	57.26	77.14
	$E_{SD} / \%$	13.33	21.43	29.75	40.45	51.67
	$E_{SS} / \%$	-1.08	-1.19	-0.86	-1.06	-0.98
	$E_{SL} / \%$	13.06	8.37	5.67	3.86	2.70

Considering both the shear deformation and the interfacial slip effect, the average computational error between the theoretical method developed in this study and ANSYS finite element method in calculating the first five order flexural natural vibration frequencies of the simply supported and fixed end CBBCW beams with the two spans, does not exceed 3.2%, and the maximum error is less than 3.3%. This is an indication that the two results are in good agreement, which shows that the theory developed in this study is correct.

The flexural natural vibration frequencies of the CBBCW increases with increase of the interface slip stiffness, but the increase rate decreases with increase of the flexural natural vibration frequency orders of the CBBCW, i.e. the interface slip effect decreases with increase of the flexural natural vibration frequency orders of the CBBCW. The interface slip effect on the CBBCW fundamental frequency is up to 13%, which cannot be neglected in the calculation.

The maximum shear deformation effect of the simply supported CBBCW is 45%, and the maximum shear deformation effect of the fixed supported end CBBCW is 63%. This is an indication that the shear deformation effect of the CBBCW is significant, i.e. the shear deformation has a significant effect on the flexural natural vibration frequency of the CBBCW, which cannot be ignored in the calculation. Further, the shear deformation effect increases significantly with the order of flexural natural vibration frequency.

The shear deformation effect of the CBBCW increases with increase of the shear connection degree, but the increase is very small. The curves between the shear deformation effect of the CBBCW beam and the flexural natural vibration frequency order under different shear connection degrees basically coincide. The results show that the shear connection degree has no significant effect on the shear deformation effect of the CBBCW.

6. Conclusions

Using the Hamilton principle and based on the factors such as the shear deformation, interfacial slip and moment of inertia, the flexural natural vibration frequency analysis method for CBBCW has been developed. By comparing the results of the analytical solution with those of the numerical solution of the finite element method, the analytical calculation method developed in this study has been proved to be correct.

The interface slip effect of the CBBCW decreases with increase of the order of the flexural natural vibration frequency, and the interface slip effect of the fundamental frequency cannot be neglected in the calculation.

The shear deformation of the CBBCW has a significant effect on the flexural natural vibration frequency, which cannot be neglected in the calculation. Further, the shear deformation effect increases significantly with increase of the order of the flexural natural vibration frequency.

The shear connection degree has little effect on the shear deformation effect of the CBBCW.

Acknowledgements

The research described in this paper was financially supported by the National Natural Science Foundations of China (51408449, 51778630), the Innovation-driven Plan in Central South University under grant (2015CX006), the independent exploration and innovation project of postgraduate in central south university (502221811).

References

- [1] Easley J T, Mcfarland D E 1969 *Journal of the Structural Division* **95** 1497-1516.
- [2] Abbas HH, Sause R, Driver RG 2007 *Journal of Structural Division* **133** 347-355.
- [3] Oh JY, Lee DH, Kim KS 2012 *Thin Wall Struct* **57** 49-61.
- [4] Zhou W, Yan W 2017 *Thin Wall Struct* **116** 201-211.
- [5] Elgaaly M, Hamilton R W, Seshadri A 1996 *J Struct Eng* **122** 390-398.
- [6] Hassanein M F, Kharoob O F 2014 *Eng Struct* **74** 157-169.
- [7] Hassanein M F, Kharoob O F 2015 *Thin Wall Struct* **88** 119-128.
- [8] Leblouba M, Junaid M T, Barakat S, Altoubat S, Maalej M 2017 *Thin Wall Struct* **113** 13-26.
- [9] Barakat S, Mansouri A A, Altoubat S 2015 *Steel Compos Struct* **18** 757-773.
- [10] Leblouba M, Barakat S, Altoubat S 2017 *J Constr Steel Res* **136** 75-90.
- [11] Sause R, Braxtan T N 2011 *J Constr Steel Res* **67** 223-236.
- [12] Nie J G, Zhu L, Tao M X 2013 *J Constr Steel Res* **85** 105-115.
- [13] Elamary A, Ahmed M M, Mohmoud A M 2017 *Eng Struct* **135** 136-148.
- [14] Zhou M, Liu Z, Zhang J 2016 *Thin Wall Struct* **109** 260-270.
- [15] He J, Liu Y, Chen A, T Y 2012 *J Constr Steel Res* **77** 193-209.
- [16] He J, Liu Y, Lin Z, Chen A, Yoda T 2012 *J Constr Steel Res* **79** 166-182.
- [17] He J, Liu Y, Chen A 2014 *Thin Wall Struct* **74** 70-84.
- [18] Nie J G, Cai C S, Zhou T R, Li Y 2007 *J Struct Eng* **133** 530-540.
- [19] Ranzi G, Zona A 2007 *Eng Struct* **29** 3026-3041.
- [20] Chakrabarti A, Sheikh A H, Griffith M, Oehlers D J 2013 *J Struct Eng* **139** 47-56.
- [21] Xu R, Wu Y 2007 *Int J Mech Sci* **49** 1139-1155.
- [22] Xu R, Wu Y 2007 *Int J Solids Struct* **44** 165-175.
- [23] Ding F, Liu J, Liu X, Guo F, Jiang L 2016 *Steel Compos Struct* **20** 1369-1389.
- [24] Liu J, Ding F, Liu X, Yu Z 2016 *Steel Compos Struct* **21** 829-847.
- [25] Jiang L, Lai Z, Zhou W 2017 *Adv Mech Eng* **9** 2071941717.
- [26] Lai Z, Jiang L, Zhou W, Chai X 2017 *Shock Vib* **2017** 1-12.
- [27] Zhou W, Jiang L, Huang Z, Li S 2016 *Steel Compos Struct* **20** 1023-1042.
- [28] Chen X C, Li Z H, Au F T K 2017 *Int J Struct Stab Dy* **17** 1750023.
- [29] Zhou W, Jiang L, Liu Z, Liu X 2012 *J Cent South Univ* **19** 2976-2982.
- [30] Zhou L, Yu Z, He G 2013 *J Cent South Univ* **20** 1354-1360.
- [31] Nie J, Cai C S, Wang T 2005 *Eng Struct* **27** 1074-1085.
- [32] Sayed-Ahmed E Y 2001 *Can J Civil Eng* **28** 656-672.
- [33] Johnson R P, Cafolla J, Bernard C 1997 *P I Civil Eng-Str B* **122** 157-164.
- [34] Zhou W, Jiang L, Yu Z 2013 *J Cent South Univ* **20** 2570-2577.